Preprints.org

Article

Not peer-reviewed version

Evidence for Proximity Effect in Superconductor-Organic Semiconductor-Superconductor Stacked DevicesEvidence for Proximity Effect in Superconductor-Organic Semiconductor-Superconductor Stacked Devices

Anna Kremen , Hagit Aviv , Yaakov Raphael Tischler * , Amos Sharoni *

Posted Date: 22 November 2024

doi: 10.20944/preprints202411.1696.v1

Keywords: proximity effect; organic light emitting diode; Niobium nitride; superconductor-LED coupling; Josephson junctions

Preprints.org is a free multidisciplinary platform providing preprint service that is dedicated to making early versions of research outputs permanently available and citable. Preprints posted at Preprints.org appear in Web of Science, Crossref, Google Scholar, Scilit, Europe PMC.

Copyright: This open access article is published under a Creative Commons CC BY 4.0 license, which permit the free download, distribution, and reuse, provided that the author and preprint are cited in any reuse.

Preprints.org (www.preprints.org) | NOT PEER-REVIEWED | Posted: 22 November 2024 doi:10.20944/preprints202411.1696.v1

Disclaimer/Publisher's Note: The statements, opinions, and data contained in all publications are solely those of the individual author(s) and contributor(s) and not of MDPI and/or the editor(s). MDPI and/or the editor(s) disclaim responsibility for any injury to people or property resulting from any ideas, methods, instructions, or products referred to in the content.

Article

Evidence for Proximity Effect in Superconductor-Organic Semiconductor-Superconductor Stacked Devices

Anna Kremen [1,2], Hagit Aviv [2,3], Yaakov Raphael Tischler [2,3,*] and Amos Sharoni [1,2,*]

[1] Department of Physics, Bar-Ilan University, Ramat-Gan 5290002, Israel
[2] Bar-Ilan Institute of Nanotechnology and Advanced Materials, Bar-Ilan University, Ramat-Gan 5290002, Israel
[3] Molecular Photonics Laboratory, Department of Chemistry, Bar-Ilan University, Ramat-Gan 5290002, Israel
* Correspondence: yaakov.tischler@biu.ac.il (Y.R.); amos.sharoni@biu.ac.il (A.S.)

Featured Application: Potentially useful for creation of correlated 2-photon entanglement.

Abstract: Coupling superconducting (SC) contacts to light-emitting layers can lead to remarkable effects, as seen in inorganic quantum-well LEDs with superconducting contacts, where an enhancement in radiative recombination was observed. Additional dramatic effects were theorized if both electrodes are SC, such as correlated emission and 2-photon entanglement. Motivated by this and by the question if proximity induced SC is possible in organic light emitting materials, we studied the electronic properties of stacked SC-organic-SC devices. Our structures consisted of Nb (bottom) and NbN (top) SC electrodes and a spin-coated light emitting semiconductor polymer, MEH-PPV. Sputtering the SC directly on the polymer causes pinhole, which we prevent by ultra-slow deposition of a 5 nm aluminum film, before depositing the top SC in-situ. The Al protects the organic film from damage and pinhole formation, while preserving SC in the top electrodes due to proximity effect between Al and NbN. Electrical transport measurements of the completed junctions indicate that indeed, the top and bottom contacts are superconducting and the protected MEH-PPV layer is pinhole-free, as supported by HR-TEM and EDS. Most important, we find that as the temperature is decreased below the critical temperature of the SCs, the device shows evidence for proximity effect in the MEH-PPV and for a Josephson effect in the device.

Keywords: proximity effect; organic light emitting diode; Niobium nitride; superconductor-LED coupling; Josephson junction

1. Introduction

When a superconducting (SC) material is brought in contact with a non-SC layer, the electronic coherence of the superconductor can be induced in the normal layer up to some penetration depth. This induction, known as the proximity effect, can result in the normal layer exhibiting the salient properties of superconductivity such as current flow for zero applied voltage [1,2]. Recently, Suemune et al. developed an inorganic LED with a SC Nb cathode and reported a dramatic increase in quantum efficiency and radiative recombination rate below TC, due to the proximity effect [3,4]. Below TC, Cooper pairs created in the Nb layer are injected into the pn-junction of the superconductor-LED (SC-LED) where they induce superradiant correlations in the radiative recombination process [5,6]. Several research teams predict that SC-LEDs will emit coherent laser-like emission with superior coherence metrics compared to traditional lasers [7–9], and discussed theoretically that SC-LEDs can be a source or detector of quantum entangled photons [10–12].

Organic materials have the potential for extraordinary process flexibility, as there is no need for crystallinity or lattice matching in order to produce a thin film of organic semiconductor that is light

© 2024 by the author(s). Distributed under a Creative Commons CC BY license.

Preprints.org (www.preprints.org) | NOT PEER-REVIEWED | Posted: 22 November 2024 doi:10.20944/preprints202411.1696.v1

emitting. Utilizing organic semiconductors can overcome some of the processing limitations in combining SC and inorganic LEDs, towards making a superconductor contacted OLED (SC-OLED).

There are two critical challenges that one must overcome before trying to realize such a device: (i) processing difficulties – can the SCs and organics retain their properties when combined in an LED geometry? (ii) is it possible to have proximity induced superconductivity in relevant organic materials? In this paper, we show both challenges are surmountable.

Combining organic materials with superconductors has been studied in a number of systems. A single island of graphene contacted laterally with W or Pb electrodes exhibited superconductivity below 1 K or around 5 K, respectively, due to the proximity effect [13,14]. Proximity effect has been also shown in single strands of DNA, CNTs, and single molecules of C60 [15–17]. Proximity effect was also investigated in conducting polymers contacted laterally by high-TC superconductors, but little effect was found due to material processing issues [18]. These studies substantiate that the proximity effect can be induced in organic materials, but there are no reports yet for proximity in thin films of light emitting semiconductors that are more suitable for a LED architecture.

Here we studied organic light emitting semiconductors that are contacted by superconducting electrodes in a vertically stacked "SC-O-SC" structure composed of a bottom SC electrode, an organic semiconductor layer, and then a top SC contact. The advantage of this architecture is that it easily expands to an OLED structure if the top SC electrode can be transparent while remaining superconducting, which we show is possible. We found evidence for proximity effect in the organic layer and Josephson junction behavior in the SC-O-SC structures, manifested by the large decrease in the layer's resistivity below the SCs' transition temperatures (TC) and the transport properties of the SC-O-SC devices.

2. Materials and Methods

A. Material considerations

We chose Nb and NbN as the contact materials because they can be fabricated without heating, oxidation or epitaxial constraints, which would destroy the organics during fabrication, in contrast to high-TC superconductors for example. Additionally, when NbN is deposited as a relatively thin layer (<15nm), it remains superconducting and is semi-transparent, thus making it a good candidate for the light transmitting electrode of the LED. In the development of transparent top-emitting OLEDs, it was shown that when sputtering a transparent cathode such as ITO on top of organics, it is beneficial to introduce a protective layer to absorb the high energy from sputtering [19,20]. Here we show that a thin layer of gently-sputtered aluminum protects the organics from the harsher and higher-rate sputtering needed to grow the top superconducting NbN. Al is also favorable since it can transfer the superconductivity, via proximity, to the semiconductor layer [21]. The organic material chosen, poly[2-methoxy-5-(2'-ethylhexyloxy)-p-phenylene vinylene] (MEH-PPV), is a fluorescent hole-transporting "p-type" semiconducting conjugated polymer, well-established for OLED fabrication [22,23].Interventionary studies involving animals or humans, and other studies that require ethical approval, must list the authority that provided approval and the corresponding ethical approval code.

B. Sample preparation

As illustrated in Figure 1a, a vertical stack of layers was chosen as the device architecture for investigating the proximity effect. To provide better heat-sinking, SC-O-SC structures were prepared on highly doped 350 μm thick Si wafers, with 0.5 μm of thermal oxide to insulate the devices electrically from the substrate. All inorganic materials were deposited using a high vacuum DC magnetron sputtering system (AJA Int.) with a base pressure of 1x10-8 Torr. Thin films of Nb (60 nm) served as the bottom electrical contact. Nb was deposited at ambient temperature from a 99.95% Nb target (ACI Alloys Inc.), in an ultra-high purity (UHP) Argon environment at a pressure of 2.4 mTorr and deposition rate of 0.18 nm/s. Electrodes were defined by depositing through a stainless-steel mechanical shadow mask with 1 mm wide lines.

Preprints.org (www.preprints.org) | NOT PEER-REVIEWED | Posted: 22 November 2024 doi:10.20944/preprints202411.1696.v1

MEH-PPV was purchased from Sigma-Aldrich (Aldrich 541443) and used without further purification. The MEH-PPV was dissolved in chloroform (Sigma-Aldrich) at a concentration of 4mg/ml, and then thin films were formed on top of the Nb layer via spin-coating in air (PMW32, Headway Research), with the conditions calibrated to yield a film thickness of 40 nm 3 nm. After spin-coating, samples were dried overnight in high vacuum (10-7 Torr) before deposition of the top electrode. Sample exposure to ambient environment during spin-coating was kept to the necessary minimum.

For the top contact layers, first a protective layer of 5 nm Al (99.99%, ACI Alloys, Inc.) was DC sputtered at a very low rate of 0.004 nm/s and 12 mTorr Argon pressure. Following, the NbN top electrode was deposited in-situ. NbN films between 15 nm to 30 nm in thickness were sputter-deposited from the Nb target in a mixed UHP Ar and Nitrogen environment of 73% and 27% respectively, at a rate of 0.04 nm/s and pressure of 2 mTorr. A cross sectional TEM of the top layers appears in Figure 1b. For patterning top electrode layers, the mechanical mask was oriented perpendicular to the bottom electrode lines, in order to create the cross junction illustrated in Figure 1c.

C. Transport measurements

Electrical transport measurements were carried out in a helium cryostat (Quantum Design PPMS) with a minimum temperature of 2K. IV characteristics were measured using a combined delta-mode setup consisting of a Keithley-6221 current source and Keithley-2182 Nano-voltmeter. The measurement configuration is illustrated in Figure 1(c). While current was passed through the junction, voltage was measured simultaneously across it (VSC-O-SC) and on the top electrode (VSC), in order to probe the state of the SC during junction activation. To minimize the effect of Joule heating, devices were measured in a pulsed delta-mode scheme [24]: current was supplied and voltage was measured during a 2 ms interval, followed by a 100 ms off-time before the next current-pulse.

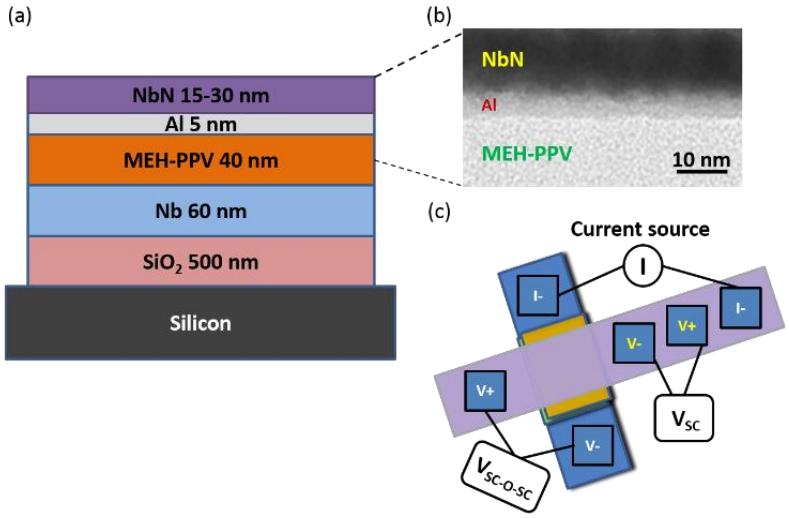

Figure 1. This is a figure. Schemes follow the same formatting. Device structure and measurement configuration. (a) Schematic of the SC-O-SC structure. Materials' order and thicknesses are marked. (b) Cross-sectional TEM focusing on the interface of MEH-PPV, Al, and NbN layers (scale bar = 10 nm). (c) Configuration of the contacts for applying current and measuring voltage simultaneously along the top superconductor and through the organic layer of the device.

D. Film characterization

A Bruker FastScan-Bio™ AFM was used to characterize morphology of the deposited layers and measure film thicknesses. The thickness of the MEH-PPV layers was also measured using a profilometer (Veeco DEKTAK 150). HR-TEM (Jeol-Jem 2100) images were acquired on cross-sections of the film stack, which were prepared by focused ion beam milling. The TEM was also used to perform position dependent Energy Dispersive Spectroscopy (EDS) to investigate the extent of layer

Preprints.org (www.preprints.org) | NOT PEER-REVIEWED | Posted: 22 November 2024 doi:10.20944/preprints202411.1696.v1

intermixing. Optical transmission measurements were obtained in a UV-Vis spectrophotometer (Cary 100 Bio UV-Vis).

3. Results and Discussion

This section may be divided by subheadings. It should provide a concise and precise description of the experimental results, their interpretation, as well as the experimental conclusions that can be drawn.

3.1. Overcoming Pinholes

Fabrication of the SC-O-SC devices requires harmonious integration of superconductors and organic materials. Deposition of the organic layer on top of the SC is very straightforward, where we can benefit from the facility of spin-coating and no need for lattice matching. AFM measurements of MEH-PPV atop Nb depicted flat layer coatings, with an RMS roughness of ~4nm and thickness of 40nm. Deposition of the top SC requires much more finesse. Sputter-deposition of NbN directly on the organic layer always resulted in Ohmic IV characteristics of the Nb/MEH-PPV/NbN junction. Cross-sectional TEM measurements of the device, Figure 2, point two contributing factors. First, the polymer was thinned to ~22 nm - half of its thickness prior to top electrode deposition, see Figure 2a. This is likely due to the heavy Nb atoms impinging the organic with enough momentum to mill into the layer. Moreover, in Figure 2(b), the local EDS measurements of Nb across the junction show an abundance of Nb atoms in the organic layer. By gently sputtering a thin layer of Al on top of MEH-PPV prior to deposition of the top superconductor, we were able to overcome these problems. As evidenced in Figure 2c, in samples with the 5 nm Al layer, the polymer thickness after NbN deposition is nearly identical to the amount initially deposited. The EDS measurements of the Al-protected junction (Figure 2d) shows that a major portion of the MEH-PPV is free of Al and Nb impurities. These findings, together with the transport properties of MEH-PPV, presented in the SC-O-SC temperature dependent transport properties section below, confirm that the Al layer is efficient in protecting the organic layer and preventing pinholes.

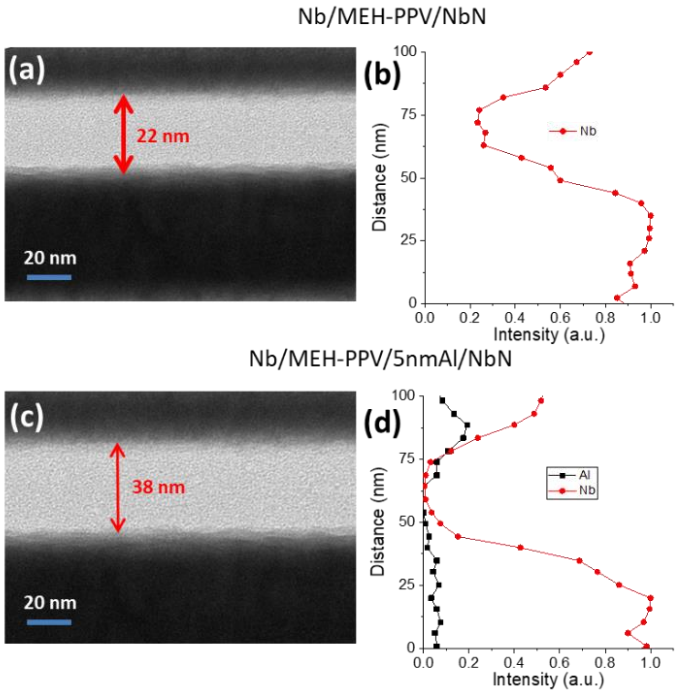

Figure 2. HR-TEM and EDS profile. (a) TEM and (b) EDS of Nb for a device without the Al layer. (c) TEM and (d) EDS of Nb and Al for a device with 5 nm Al protective layer.

Preprints.org (www.preprints.org) | NOT PEER-REVIEWED | Posted: 22 November 2024 doi:10.20944/preprints202411.1696.v1

3.2. Superconductors' Properties

The SC critical temperatures of the bottom Nb electrode, deposited on silicon, and spin-coated with MEH-PPV on top was ~8.2 K, see Figure 3a. The transition width (from 90% to 10% of normal resistance) was 0.05K, and the normal resistance was 2.7 Ω/ near TC. Thus, the spin- coating does not affect the bulk Nb properties, but this measurement does not rule out possible interface degradation. In Figure 3b we compare resistance vs. temperature measurements of 15 nm NbN films deposited on silicon or on top of the MEH-PPV(40 nm)/Al(5 nm) layers. The TC slightly decreased, from 10.01 K to 9.90 K, when depositing on the organic. These are lower than the reported TC~17 K of NbN, but reasonable considering the imposed deposition conditions, i.e. room temperature deposition, low rate and thickness. The transition width increased from 0.88 K for NbN on Si to 1.06 K when deposited on MEH-PPV. For temperatures just above TC, the resistance for NbN on MEH-PPV/Al is 20% higher than on Si. NbN acts like a "bad metal", in that its resistivity increases with decreasing temperature (in our films from room temperature resistance of ~ 115 Ω/ , to ~ 160 Ω/ for temperatures just above TC). The critical currents of the NbN (15 nm) top electrodes, measured for several temperatures below TC, plotted in Figure 3c, show linear increase with decreasing temperature. The critical current density is approximately an order of magnitude lower than observed for clean NbN. Finally, the optical transmission spectrum was measured for a Al(5 nm)/NbN(15 nm) bilayer, deposited on a glass substrate simultaneously with the MEH-PPV/Al/NbN sample described above, see Figure 3d. More than 27% of incident light is transmitted through the top Al/NbN electrode.

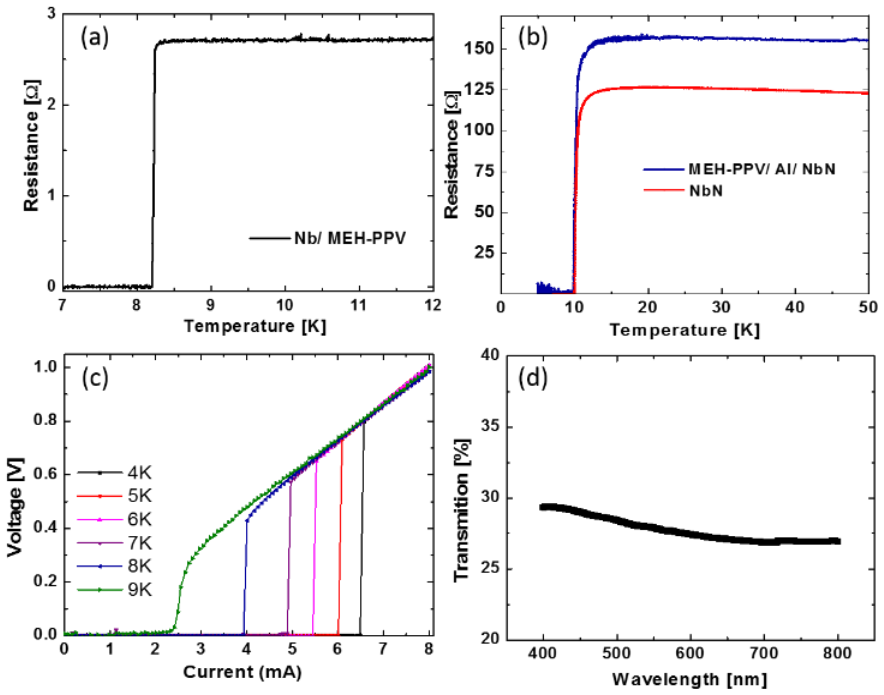

Figure 3. Characterization of superconducting layers. (a) Resistance vs. temperature of Nb film (50 nm) spin-coated with MEH-PPV. (b) Resistance vs. temperature of NbN film (15 nm) deposited on Si substrate (red) and MEH-PPV/Al (blue) (c) Voltage vs. current across the NbN layer, showing critical current at different temperatures. (d) Optical transmission through a Al(5 nm)/ NbN(15 nm) bilayer deposited on a glass substrate.

3.3. SC-O-SC Temperature Dependent Transport Properties

In Figure 4, we present temperature dependent IV measurements of the SC-O-SC devices depicted in Figure 1a, with 5nm Al and 30 nm thick NbN. We use a thicker NbN electrode to strengthen its SC properties (e.g., TC increased to 11.4 K in this device) and proximity effect, since the main goal was to search for SC signatures in the transport properties of the junctions.

Preprints.org (www.preprints.org) | NOT PEER-REVIEWED | Posted: 22 November 2024 doi:10.20944/preprints202411.1696.v1

The IV at 300 K shows non-linear current increase with voltage, similar to previously reported for MEH-PPV junctions, indicating space charge limited conductivity [25]. As the temperature is lowered, the resistivity of the organic layer increases, providing further evidence that the metal-semiconductor-metal device is not governed by pinholes.

Looking at the IV behavior just below the NbN transition temperature, one observes a region with negative differential resistance (NDR) above 8 mA, blue curve in Figure 4, measured at 11 K. By comparing (inset of Figure 4) the voltage drop on the NbN electrode (purple) with the voltage across the SC-O-SC junction (blue), as a function of current, we observe that the NDR coincides with crossing the SC critical current of NbN. This behavior is expected, recalling that when NbN becomes normal there is excess Joule heating, due to the relatively high resistance of NbN [26], which increases at low temperatures. This means that upon reaching the critical current, dissipation in NbN contributes to the temperature increase of the junction, therefore lowering the resistance of the MEH-PPV. This also explains the difference in the MEH-PPV high voltage characteristics when comparing the measurements at 15 K and higher temperatures with those at temperatures below 11 K. Evidently, when measuring with larger currents and above 15 K, Joule heating of the NbN heats the MEH-PPV and changes its IV measurement. For temperatures below 11 K, the NbN is superconducting and there is no excess heating of the junction. Thus, the junction temperature is lower, and the organic's resistance is higher.

We note in passing that we have also measured light emitting properties in a similar OLED device through the top electrode, where an additional inorganic blocking layer was added, see Supplemental Material for details[27]. This device showed light emission down to the lowest temperature measured of 5 K. This provides further support for the effectiveness of Al in preventing damage to the organic layer, since emission would be strongly quenched if pinholes were present.

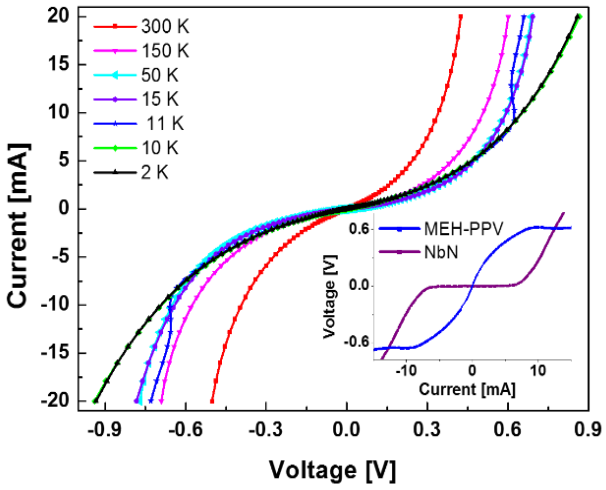

Figure 4. Current vs. voltage of the SC-O-SC junction for temperatures between 2 K to 300 K. IV curves show space charge limited conductivity for the MEH-PPV layer. Inset: V vs. I measured at 11 K for NbN (purple) and MEH-PPV (blue). NbN displays a critical current of 8 mA. The onset of negative differential resistance in the device corresponds with the critical current.

Figure 5 presents the main results of our study. In Figure 5a we plot the low bias resistance of the SC-O-SC junction as a function of temperature (normalized to the maximal resistance). There is a considerable drop in resistance coinciding with the critical temperature of NbN (11.4 K, right dotted line), then there is a further resistance drop upon crossing the Nb critical temperature (8.1 K, left dotted line). The final resistance, however, is not zero, reaching 10% of the maximum resistance at our lowest attainable temperature of 2K.

Figure 5b provides a zoomed in view, up to 12 mV, of the IV curves for temperatures between 2 K and 11 K. Generally, for these small currents, the organic semiconductor is in the ohmic regime, and far from the space charge limited behavior that we observed at higher voltages (Figure 5) that is common in polymers such as MEH-PPV [25]. For all temperatures above 11 K, the behavior is ohmic,

Preprints.org (www.preprints.org) | NOT PEER-REVIEWED | Posted: 22 November 2024 doi:10.20944/preprints202411.1696.v1

but also for temperatures above 8K the behavior is nearly ohmic. Below 8 K, the TC of Nb, the IV characteristics change considerably and show features typical for the onset of the Josephson effect[28]. The Josephson critical current, i.e. the current at which the resistance changes back to the normal ohmic regime, increases with temperature and is shifted relative to the normal behavior, see inset of Figure 5b.

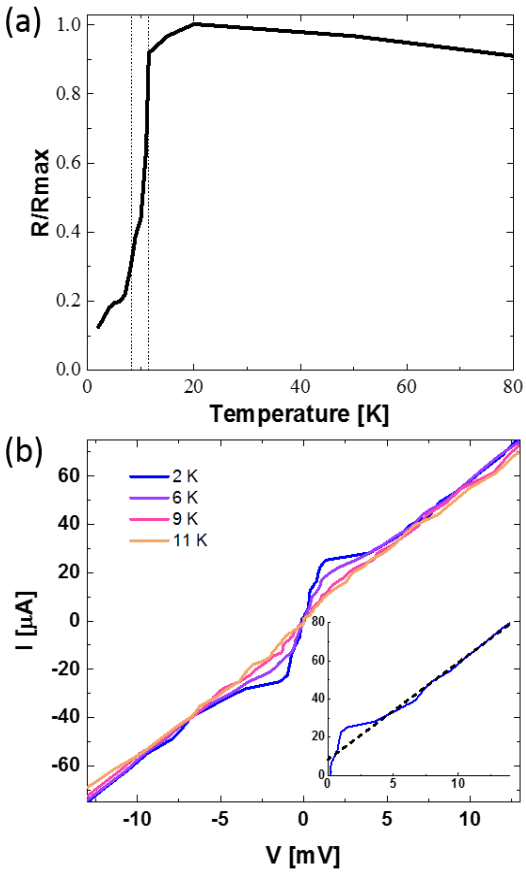

Figure 5. Low voltage and low temperature measurements. (a) Normalized zero bias resistance vs. temperature of the SC-O-SC stack. Dotted lines mark the TC of NbN (11.4 K) and Nb (8.1 K) electrodes. (b) main – Low voltage IV measurements at temperatures between 2 K and 11 K, as marked. Inset – IV measured at 2 K. The dotted line extrapolates the linear IV regime to 0 V with non-zero residual current, indicative of a Josephson junction.

Similar IV behavior was reported in studies on proximity induced superconductivity in conventional semiconducting materials [21,29–31] and also in lateral devices of organic semiconducting nano-items such as individual single wall carbon nanotubes [16], DNA strands [15] and graphene nano-islands [14]. In these studies, the critical temperature for the appearance of a Josephson critical current was usually below 0.5K (using similar superconductors), which is lower than the temperatures attainable in our cryostat which has a base-temperature of 2K. When these samples were at temperatures above ~ 0.5 K and yet below TC of the superconducting contacts, the resistivity decreased as the temperature was lowered but did not drop to zero, consistent with the trends we observe in our results.

4. Conclusions

In conclusion, we successfully integrated superconductors and organic materials in a vertically stacked structure by adding a protective Al layer prior to the harsher deposition of the top NbN electrode. We demonstrated that transport properties of the SC-O-SC devices consisting of Nb/MEH-PPV/Al/NbN are not due to pinholes: (i) EDS measurements depicted a significant metal-free organic

Preprints.org (www.preprints.org) | NOT PEER-REVIEWED | Posted: 22 November 2024 doi:10.20944/preprints202411.1696.v1

layer; (ii) the junctions show typical space-charge limited IV characteristics of single layer organic semiconductor structures; (iii) the junction resistance increases as the temperature is lowered, down to temperatures just above the NbN TC; and (iv) a similar junction with an additional V2O5 blocking layer had light emitting properties down to the lowest temperatures.

At temperatures below the TC of NbN the onset of proximity induced superconductivity in the MEH-PPV layer is manifest. The zero-bias resistance across the junction reduces significantly with temperature following the superconducting transitions of both the Nb and NbN electrodes. Our measurements were performed at temperatures higher than 2 K. Given these results, it is reasonable to estimate that complete Josephson current could be realized at lower temperatures or by reducing the voltage noise of the low current measurements.

The stacked architecture we developed can serve as a platform for fabrication and investigation of SC-OLEDs. Our measurements show proximity induced coherence in p-type MEH-PPV layers, and suggest that these effects should be observable in other organic semiconductor thin films, at low but accessible temperatures. In addition, we successfully created a semi-transparent and superconducting top electrode. Thus, we have presented a flexible framework in which to study and observe the role of superconductor induced coherence on the excitonic properties of organic light emitting materials. Such coherence effects could have a pronounced impact on exciton formation and recombination and ultimately lead to brighter or even laser-like coherent emission upon electrical excitation, a goal sought elusively from many directions for organic semiconductors [32,33]

Supplementary Materials: The following supporting information can be downloaded at the website of this paper posted on Preprints.org, Figure S1: Electroluminescence at low temperature.

Funding: This research was partially funded by MOST-SFF #6068.

Data Availability Statement: The raw data that support the findings of this study are available from the corresponding authors upon reasonable request.

Acknowledgments: The authors would like to thank Yafit Fleger and Judith Grinblat for their help with FIB and TEM, Itamar Padal for assistance with electrical wiring of the cryostat and Yehonathan Ramon for assistance with profilometry. The authors are grateful to Prof. Benny Ehrenberg for providing the first batch of MEH-PPV.

Conflicts of Interest: The authors declare no conflicts of interest. The funders had no role in the design of the study; in the collection, analyses, or interpretation of data; in the writing of the manuscript; or in the decision to publish the results.

References

1. Josephson, B.D. Potential differences in the mixed state of type II superconductors. *Phys. Letters* **1965**, *16*, 1963-1964.
2. Bouscher, S.; Panna, D.; Balasubramanian, K.; Cohen, S.; Ritter, D.; Hayat, A. Enhanced Cooper-Pair Injection into a Semiconductor Structure by Resonant Tunneling. *Phys. Rev. Lett.* **2022**, *128*, 127701, doi:10.1103/physrevlett.128.127701.
3. Suemune, I.; Sasakura, H.; Hayashi, Y.; Tanaka, K.; Akazaki, T.; Asano, Y.; Inoue, R.; Takayanagi, H.; Hanamura, E.; Huh, J.-H.; et al. Cooper-Pair Radiative Recombination in Semiconductor Heterostructures: Impact on Quantum Optics and Optoelectronics. *Japanese Journal of Applied Physics* **2012**, *51*, 010114.
4. Mou, S.S.; Irie, H.; Asano, Y.; Akahane, K.; Nakajima, H.; Kumano, H.; Sasaki, M.; Murayama, A.; Suemune, I. Optical observation of superconducting density of states in luminescence spectra of InAs quantum dots. *Physical Review B* **2015**, *92*, 035308.
5. Asano, Y.; Suemune, I.; Takayanagi, H.; Hanamura, E. Luminescence of a Cooper Pair. *Phys. Rev. Lett.* **2009**, *103*, 4, doi:18700110.1103/PhysRevLett.103.187001.
6. Sasakura, H.; Kuramitsu, S.; Hayashi, Y.; Tanaka, K.; Akazaki, T.; Hanamura, E.; Inoue, R.; Takayanagi, H.; Asano, Y.; Hermannstädter, C.; et al. Enhanced Photon Generation in a Nb/n-InGaAs/p-InP Superconductor/Semiconductor-Diode Light Emitting Device. *Phys. Rev. Lett.* **2011**, *107*, 157403.
7. Benz, S.P.; Burroughs, C.J. Coherent emission from two-dimensional Josephson junction arrays. *Applied Physics Letters* **1991**, *58*, 2162-2164, doi:doi:http://dx.doi.org/10.1063/1.104993.

Preprints.org (www.preprints.org) | NOT PEER-REVIEWED | Posted: 22 November 2024 doi:10.20944/preprints202411.1696.v1

8. Ozyuzer, L.; Koshelev, A.E.; Kurter, C.; Gopalsami, N.; Li, Q.; Tachiki, M.; Kadowaki, K.; Yamamoto, T.; Minami, H.; Yamaguchi, H.; et al. Emission of Coherent THz Radiation from Superconductors. *Science* **2007**, *318*, 1291-1293, doi:10.1126/science.1149802.
9. Godschalk, F.; Hassler, F.; Nazarov, Y.V. Proposal for an Optical Laser Producing Light at Half the Josephson Frequency. *Phys. Rev. Lett.* **2011**, *107*, 073901.
10. Recher, P.; Nazarov, Y.V.; Kouwenhoven, L.P. Josephson Light-Emitting Diode. *Phys. Rev. Lett.* **2010**, *104*, 156802, doi:10.1103/PhysRevLett.104.156802.
11. Bouscher, S.; Panna, D.; Hayat, A. Semiconductor–superconductor optoelectronic devices. *Journal of Optics* **2017**, *19*, 103003.
12. Hayat, A.; Kee, H.-Y.; Burch, K.S.; Steinberg, A.M. Cooper-pair-based photon entanglement without isolated emitters. *Physical Review B* **2014**, *89*, doi:10.1103/physrevb.89.094508.
13. Shailos, A.; Nativel, W.; Kasumov, A.; Collet, C.; Ferrier, M.; Guéron, S.; Deblock, R.; Bouchiat, H. Proximity effect and multiple Andreev reflections in few-layer graphene. *Europhysics Letters* **2007**, *79*, 57008.
14. Borzenets, I.V.; Coskun, U.C.; Jones, S.J.; Finkelstein, G. Phase Diffusion in Graphene-Based Josephson Junctions. *Phys. Rev. Lett.* **2011**, *107*, 137005.
15. Kasumov, A.Y.; Kociak, M.; Guéron, S.; Reulet, B.; Volkov, V.T.; Klinov, D.V.; Bouchiat, H. Proximity-Induced Superconductivity in DNA. *Science* **2001**, *291*, 280-282, doi:10.1126/science.291.5502.280.
16. Kasumov, a.Y. Supercurrents Through Single-Walled Carbon Nanotubes. *Science* **1999**, *284*, 1508-1511, doi:10.1126/science.284.5419.1508.
17. Winkelmann, C.B.; Roch, N.; Wernsdorfer, W.; Bouchiat, V.; Balestro, F. Superconductivity in a single-C60 transistor. *Nat Phys* **2009**, *5*, 876-879, doi:10.1038/nphys1433.
18. Haupt, S.G.; Riley, D.R.; Jones, C.T.; Zhao, J.; McDevitt, J.T. Reversible modulation of Tc in conductive polymer/high temperature superconductor assemblies. *Journal of the American Chemical Society* **1993**, *115*, 1196-1198, doi:10.1021/ja00056a082.
19. Chen, H.; Qiu, C.; Wong, M.; Kwok, H.S. DC sputtered indium-tin oxide transparent cathode for organic light-emitting diode. *IEEE Electron Device Letters* **2003**, *24*, 315-317.
20. Gu, G.; Bulović, V.; Burrows, P.E.; Forrest, S.R.; Thompson, M.E. Transparent organic light emitting devices. *Applied Physics Letters* **1996**, *68*, 2606-2608, doi:doi:http://dx.doi.org/10.1063/1.116196.
21. Drachmann, A.C.C.; Suominen, H.J.; Kjaergaard, M.; Shojaei, B.; Palmstrøm, C.J.; Marcus, C.M.; Nichele, F. Proximity Effect Transfer from NbTi into a Semiconductor Heterostructure via Epitaxial Aluminum. *Nano Letters* **2017**, *17*, 1200-1203, doi:10.1021/acs.nanolett.6b04964.
22. Ju, J.; Yamagata, Y.; Higuchi, T. Thin-Film Fabrication Method for Organic Light-Emitting Diodes Using Electrospray Deposition. *Advanced Materials* **2009**, *21*, 4343-4347, doi:10.1002/adma.200900444.
23. Zhao, X.; Zhan, X. Electron transporting semiconducting polymers in organic electronics. *Chemical Society Reviews* **2011**, *40*, 3728-3743, doi:10.1039/C0CS00194E.
24. Daire, A.; Goeke, W.; Tupta, M.A. White paper: new instruments can lock out lock-ins. Available online: http://www.keithley.com/data?asset=50379 (accessed on
25. Reddy, V.S.; Dhar, a. Optical and charge carrier transport properties of polymer light emitting diodes based on MEH-PPV. *Physica B: Condensed Matter* **2010**, *405*, 1596-1602, doi:10.1016/j.physb.2009.12.048.
26. Chand, M.; Mishra, A.; Xiong, Y.; Kamlapure, A.; Chockalingam, S.; Jesudasan, J.; Bagwe, V.; Mondal, M.; Adams, P.; Tripathi, V.; et al. Temperature dependence of resistivity and Hall coefficient in strongly disordered NbN thin films. *Physical Review B* **2009**, *80*, 134514, doi:10.1103/PhysRevB.80.134514.
27. See Supplemental Material at http for the light emmiting properties of the modified OLED with SC contacts.
28. Waldram, J.R.; Pippard, A.B.; Clarke, J. Theory of the Current-Voltage Characteristics of SNS Junctions and other Superconducting Weak Links. *Philosophical Transactions of the Royal Society of London. Series A, Mathematical and Physical Sciences* **1970**, *268*, 265-287, doi:10.1098/rsta.1970.0075.
29. Magnée, P.H.C.; van der Post, N.; Kooistra, P.H.M.; van Wees, B.J.; Klapwijk, T.M. Enhanced conductance near zero voltage bias in mesoscopic superconductor-semiconductor junctions. *Physical Review B* **1994**, *50*, 4594-4599.
30. Aly, A.H.; Phillips, A.H. Quantum Transport in a Superconductor-Semiconductor Mesoscopic System. *Physica Status Solidi (B)* **2002**, *232*, 283-287, doi:10.1002/1521-3951(200208)232:2<283::AID-PSSB283>3.0.CO;2-G.

Preprints.org (www.preprints.org) | NOT PEER-REVIEWED | Posted: 22 November 2024 doi:10.20944/preprints202411.1696.v1

31. Paajaste, J.; Amado, M.; Roddaro, S.; Bergeret, F.S.; Ercolani, D.; Sorba, L.; Giazotto, F. Pb/InAs Nanowire Josephson Junction with High Critical Current and Magnetic Flux Focusing. *Nano Letters* **2015**, *15*, 1803-1808, doi:10.1021/nl504544s.
32. Wegmann, G.; Giessen, H.; Greiner, A.; Mahrt, R.F. Laser emission from a solid conjugated polymer: Gain, tunability, and coherence. *Physical Review B* **1998**, *57*, R4218-R4221.
33. Samuel, I.D.W.; Turnbull, G.A. Organic semiconductor lasers. *Chemical reviews* **2007**, *107*, 1272-1295, doi:10.1021/cr050152i.

Disclaimer/Publisher's Note: The statements, opinions and data contained in all publications are solely those of the individual author(s) and contributor(s) and not of MDPI and/or the editor(s). MDPI and/or the editor(s) disclaim responsibility for any injury to people or property resulting from any ideas, methods, instructions or products referred to in the content.